Title
Free Electron Laser Lithotripsy: Threshold Radiant Exposures

Journal
Journal of Endourology, 14(2)

ISSN
0892-7790

Authors
Chan, KF
Hammer, DX
Choi, B
et al.

Publication Date
2000-03-01

DOI
10.1089/end.2000.14.161

JOURNAL OF ENDOUROLOGY
Volume 14, Number 2, March 2000
Mary Ann Liebert, Inc.

Free Electron Laser Lithotripsy: Threshold Radiant Exposures

KIN FOONG CHAN, M.S.E.,[1] DANIEL X. HAMMER, M.S.E.,[1] BERNARD CHOI, M.S.E.,[2] JOEL M.H. TEICHMAN, M.D., FRCSC,[3] H. STAN McGUFF, D.D.S.,[4] HANS PRATISTO, Ph.D.,[5] E. DUCO JANSEN, Ph.D.,[5] and ASHLEY J. WELCH, Ph.D.[1,2]

ABSTRACT

Purpose: **To determine the threshold radiant exposures (J/cm^2) needed for ablation or fragmentation as a function of infrared wavelengths on various urinary calculi and to determine if there is a relation between these thresholds and lithotripsy efficiencies with respect to optical absorption coefficients.**

Materials and Methods: **Human calculi composed of uric acid, calcium oxalate monohydrate (COM), cystine, or magnesium ammonium phosphate hexahydrate (MAPH) were used. The calculi were irradiated in air with the free electron laser (FEL) at six wavelengths: 2.12, 2.5, 2.94, 3.13, 5, and 6.45 μm.**

Results: **Threshold radiant exposures increased as optical absorption decreased. At the near-infrared wavelengths with low optical absorption, the thresholds were >1.5 J/cm^2. The thresholds decreased below 0.5 J/cm^2 for regions of high absorption for all the calculus types. Thresholds within the high-absorption regions were statistically different from those in the low-absorption regions, with *P* values much less than 0.05.**

Conclusions: **Optical absorption coefficients or threshold radiant exposures can be used to predict lithotripsy efficiencies. For low ablation thresholds, smaller radiant exposures were required to achieve breakdown temperatures or to exceed the dynamic tensile strength of the material. Therefore, more energy is available for fragmentation, resulting in higher lithotripsy efficiencies.**

INTRODUCTION

LASERS HAVE BEEN USED EXTENSIVELY for fragmenting urinary[1–8] and biliary[9–11] calculi. The fragmentation mechanism for the Q-switched Nd:YAG and pulsed-dye lasers is predominantly photomechanical or photoacoustical.[12] In the former, both optical breakdown of water and bubble collapse generate shockwaves on the order of 100 bar that fragment the calculus.[13–15] In the latter, plasma expansion generates a smaller shockwave than is produced by the bubble collapse, and this second shockwave produces calculus fragmentation.[7,14,15]

Recently, the long pulsed Ho:YAG laser (λ = 2.12 μm) has become popular for clinical lithotripsy.[16–23] The fragmentation mechanism is predominantly photothermal, with concomitant chemical breakdown of the irradiated calculus.[11,24–27] The Ho:YAG laser has a penetration depth of about 400 μm in water and a pulse duration of 250 μsec that provides thermal confinement within the irradiated water and calculus volume. As a result, calculus fragmentation is highly localized and directional.[21,22] This condition effectively minimizes or prevents collateral tissue damage. In addition, the ablation process yields smaller fragments, allowing easier passage through the urinary tract.[28]

The thermal fragmentation process by the Ho:YAG laser suggests that other wavelengths in the infrared spectrum might be more efficient for calculus fragmentation. Daidoh and associates[29] predict that the optimum wavelengths for fragmentation may occur at the major optical absorption peaks of uric acid and calcium oxalate monohydrate (COM) calculi at 3 μm and 6 μm. Chan and coworkers[30] have shown that the fragmentation efficiencies are higher at 3.13 μm and 6.1 μm than at the holmium wavelength of 2.12 μm for these two types of calculi. However, the dependence of fragmentation efficiency on the optical absorption coefficient has not been confirmed.

Assuming a photothermal fragmentation mechanism similar to that of the Ho:YAG laser with no heat conduction beyond the irradiated calculus volume (which is a good assumption for laser pulse durations less than a few hundred microseconds), the relation for threshold radiant exposure for ablation[31] is

[1]Department of Electrical and Computer Engineering and [2]Biomedical Engineering Program, The University of Texas at Austin, Austin, Texas.
[3]Division of Urology and [4]Division of Dentistry, The University of Texas Health Science Center, San Antonio, Texas.
[5]Department of Biomedical Engineering, Vanderbilt University, Nashville, Tennessee.

$$H_{th} = \frac{\rho c \Delta T}{\mu_a} \text{ [J/cm}^2\text{]} \quad (1)$$

where H_{th} is the threshold radiant exposure (J/cm^2), ρ is the material density (kg/cm^3), and c is the material-specific heat (J/kg°C), ΔT is the difference between the breakdown temperature and the ambient temperature (°C), and μ_a is the optical absorption coefficient (cm^{-1}). Equation 1 implies that the threshold radiant exposure for ablation or fragmentation is inversely proportional to the optical absorption coefficient.

In this study, we measured the threshold radiant exposures of various urinary calculi at different wavelengths selected within the infrared spectral regions with low absorption and high absorption (Fig. 1). As shown for this example, 2.94, 3.13, 5, and 6.45 μm fall within the high-absorption regions around the absorption peaks in the 3.3-μm and 6-μm ranges, whereas 2.12 and 2.5 μm fall within the near-infrared low-absorption region (λ <2.7 μm). No measurement was performed in the mid-infrared low-absorption region (4.1 μm $< \lambda <$ 4.8 μm). According to equation 1, one expects 2.94, 3.13, 5, and 6.45 μm to exhibit low ablation thresholds and 2.12 and 2.5 μm to show high ablation thresholds. Note that 2.12 μm is equivalent to the wavelength of the Ho:YAG laser used as a reference in our study, and 2.94 μm is equivalent to the Er:YAG laser wavelength.

MATERIALS AND METHODS

Specimens

Human calculi composed of >95% uric acid, >95% cystine, >95% COM, and >90% magnesium ammonium phosphate hexahydrate (MAPH) were obtained from a stone analysis laboratory (Louis C. Herring Co., Orlando, FL). The calculi were cut with a dental diamond saw to produce a flat surface for laser irradiation.

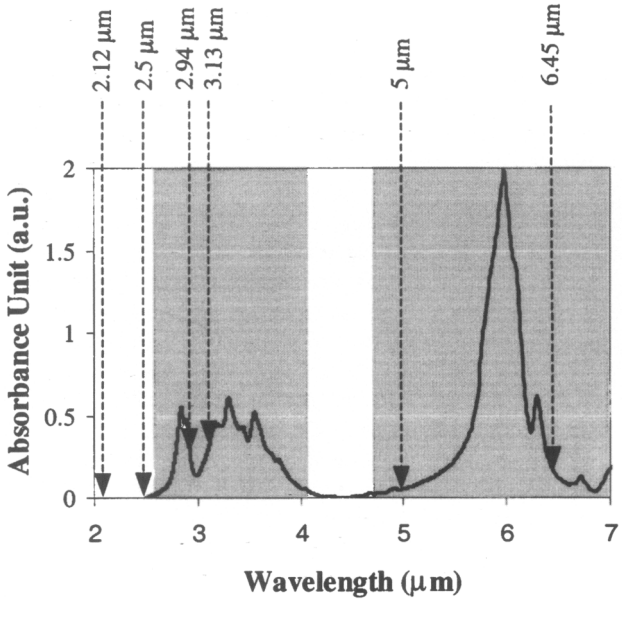

FIG. 1. Absorption spectrum of uric acid calculi (from reference 34). Arrows indicate wavelengths at which experiments were conducted. Shaded areas are optical high-absorption regions.

Free electron laser

The FEL (Vanderbilt University, Nashville, TN) with tunable wavelengths from 2 to 10 μm and a macropulse duration from 3 to 5 μsec (full-width–half-maximum) was used in the study. The macropulse consisted of a train of picosecond micropulses. Each pair of micropulses was separated by a 350-psec interval; a total of 17,000 micropulses formed a macropulse. A maximum repetition rate of 30 macropulses/sec was available. In our experiments, single macropulses were used. Six wavelengths were involved in the study: 2.12, 2.5, 2.94, 3.13, 5, and 6.45 μm. The wavelengths were associated with either the spectral regions of low or high absorption for the various types of urinary calculi (see Figs. 4 through 7 below).

Threshold radiant exposure for ablation or fragmentation

The ablation threshold was defined as the minimum laser energy per unit area (J/cm^2) required to produce visual damage on the calculus surface. A double-blind study was performed in which the laser energy was varied above, at, and below the thresholds for ablation unknown to the observer. The experimental set-up for irradiation of the calculi is shown in Figure 2. Initially, the energy ratio between the target and the reference was measured. During the experiment, the energy measured at the reference was used to determine the energy at the target. The laser spot size at the calculus surface was measured with the knife-edge technique.[32] Spot diameters ranged from 185 μm to 310 μm. Typically, the spot diameter increased with wavelength. The spot area and the laser energy were used to calculate the radiant exposure. Random levels of single-shot laser energy were delivered to a 7 × 7 grid on the calculus surface (Fig. 2). The observation of either ablation or no ablation for a maximum of 49 single pulses was processed using probit analysis.[33] The estimated dose for a 50% probability of ablation (ED_{50}) values of the probit curves were specified as the threshold radiant exposures (Fig. 3).

For all compositions, the threshold results were categorized by wavelength into three groups: within the high-absorption spectral regions, the near-infrared low-absorption region, or the mid-infrared low-absorption region. Student's *t*-tests were performed to test the null hypothesis that the first group is statistically similar to the latter two groups. A P value <0.05 was considered significant for rejecting the hypothesis (unequal).

RESULTS

Figures 4 to 7 show the results of the threshold radiant exposure measurements using probit analysis for the uric acid, COM, cystine, and MAPH calculi. Also shown in each figure is the calculus absorption spectrum, described as the relative absorbance in arbitrary units,[34] not to be confused with the absorption coefficient in cm^{-1}. Regions of low absorption are indicated in white, and high absorption regions are shaded. For

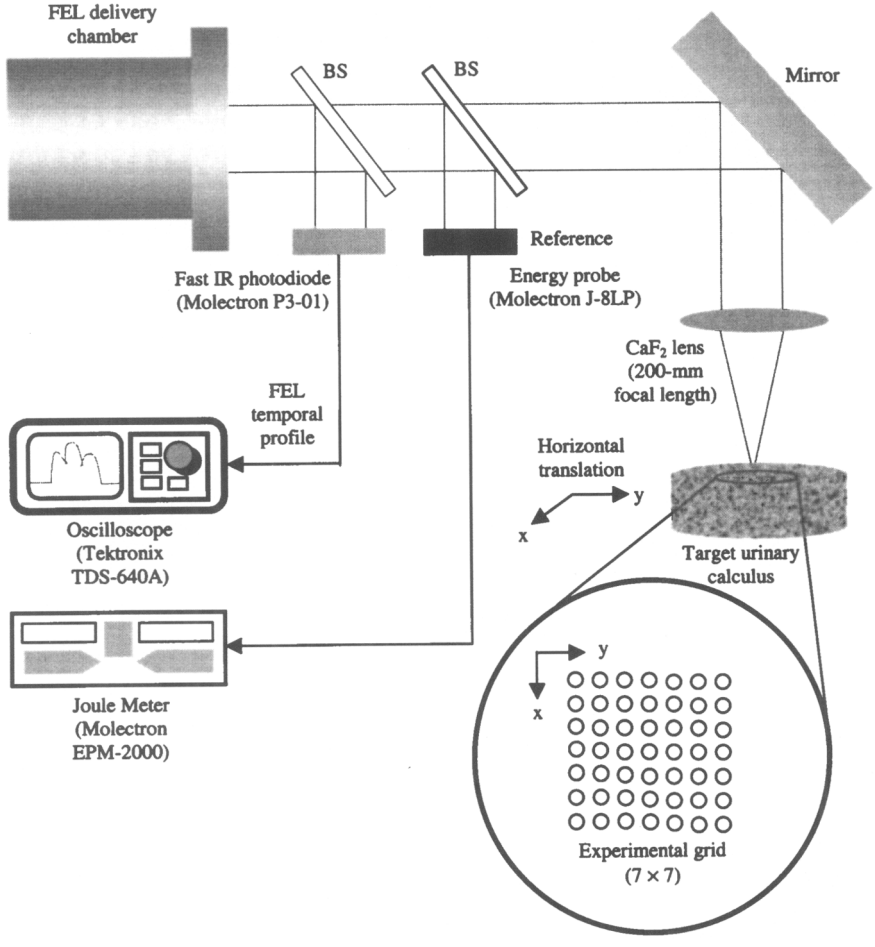

FIG. 2. Experimental set-up for measurement of ablation threshold at different wavelengths for various types of calculi. BS = beamsplitter.

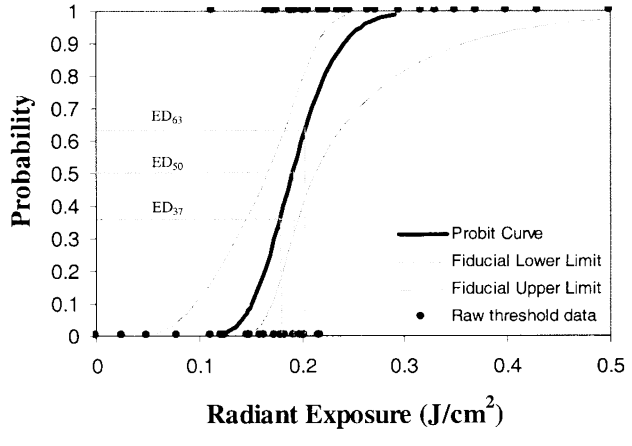

FIG. 3. Example of probit curve for uric acid calculus at 3.13 μm. Fiducial limits, which express confidence interval, were set at 95% for all calculations. Curve shows probability of ablation as function of radiant exposure (J/cm^2). Threshold radiant exposure is defined as value at which probability of ablation is 50% (estimated dose; ED_{50}), which in this case is H_{th} = 0.19 J/cm^2. Radiant exposures at ED_{37} and ED_{63} are used as lower and upper bound, respectively, of error bars in Figures 4 through 7.

uric acid calculi (Fig. 4), the threshold radiant exposures were 0.18, 0.19, 0.5, and 0.28 J/cm^2 at 2.94, 3.13, 5, and 6.45 μm, respectively, in the high-absorption regions. The thresholds increased to approximately 3.7 J/cm^2 and 3.8 J/cm^2 at 2.12 μm and 2.5 μm, respectively, in the near-infrared low-absorption region. Similar trends were observed for all compositions, where in general, high optical absorption resulted in low threshold radiant exposures and vice versa (Table 1; Figs. 4 through 7). In COM and MAPH calculi, however, the thresholds at 5 μm were not at levels comparable to those at 2.12 and 2.5 μm (Figs. 5 and 7). In fact, the threshold at 5 μm was lower than that at 6.45 μm for the MAPH calculus. Relatively low absorption at 2.94 μm by the cystine calculus also did not correspond to a marked increase in ablation threshold (Fig. 6). Statistical analysis confirmed that the threshold radiant exposures in the spectral regions of high absorption were statistically different from those in the near- and mid-infrared regions.

DISCUSSIONS

This study demonstrated that the ablation threshold of urinary calculi is dependent on the optical absorption. The opti-

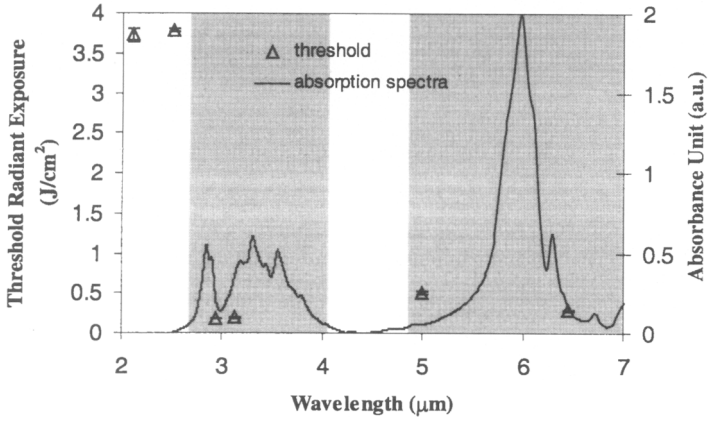

Calculus	Near-IR Absorption Region ($\lambda < 2.7$ μm)	Mid-IR Absorption Region (4.1 μm $< \lambda <$ 4.8 μm)
Uric Acid	$p = 8.69466 \times 10^{-11}$ ($p < 0.05$)	N/A

FIG. 4. Threshold radiant exposure results for uric acid calculus. At top are threshold values and error bars as defined in legend to Figure 3. Absorption spectrum of calculus is superimposed on results. Shaded areas are regions of high optical absorption. At bottom are *P* values for threshold radiant exposures in infrared high-absorption regions compared with near-infrared low-absorption and mid-infrared low- absorption regions. NA = no data available for analysis.

mum wavelength (or the lowest threshold) for fragmentation occurred primarily in the infrared regions known to have high optical absorption by all calculi used in this study: 2.94, 3.13, 5, and 6.45 μm for the uric acid calculus; 2.94, 3.13, and 6.45 μm for the COM and MAPH calculi; and 3.13, 5, and 6.45 μm for the cystine calculus.

Our results are consistent with those of Daidoh and coworkers,[29] who suggested that the optimum wavelengths for fragmentation of both uric acid and COM calculi were at 3 μm and 6 μm. Dretler[6] has shown an increase in fragmentation threshold with increased wavelength for MAPH and calcium oxalate calculi using a tunable pulsed-dye laser (λ = 445, 504, and 577 nm). However, these results have not been compared with calculus absorption. Coincidentally, Long and coworkers[35] have reported a decrease in absorption coefficient with increased wavelength for pigmented biliary calculi in the visible spectrum between 488 nm and 630 nm. Unfortunately, the compositions of the biliary calculi are not known. It is not clear if the relation between the ablation threshold and absorption coefficient found in this paper extends to the visible region (assuming similar compositions), although the studies of Dretler and Long et al. indicate that they may.

Calculus fragmentation at infrared wavelengths is mainly photothermal.[30] Our ablation threshold measurements follow a trend suggested by equation 1, whereby an increase in the absorption coefficient results in a decrease in the threshold. A

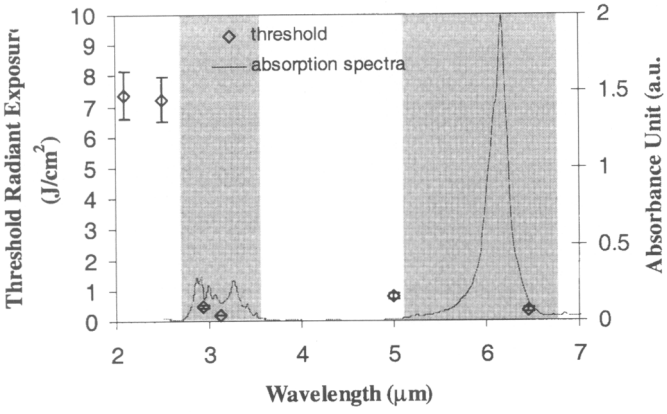

Calculus	Near-IR Absorption Region ($\lambda < 2.7$ μm)	Mid-IR Absorption Region (3.5 μm $< \lambda <$ 5.1 μm)
COM	$p = 7.22159 \times 10^{-11}$ ($p < 0.05$)	$p = 1.23704 \times 10^{-10}$ ($p < 0.05$)

FIG. 5. Threshold radiant exposure results for COM calculus. At top are threshold values and error bars as defined in legend to Figure 3. Absorption spectrum of calculus is superimposed on results. Shaded areas are regions of high optical absorption. At bottom are *P* values for threshold radiant exposures in infrared high-absorption regions compared with near-infrared low-absorption and mid-infrared low- absorption regions. NA = no data available for analysis.

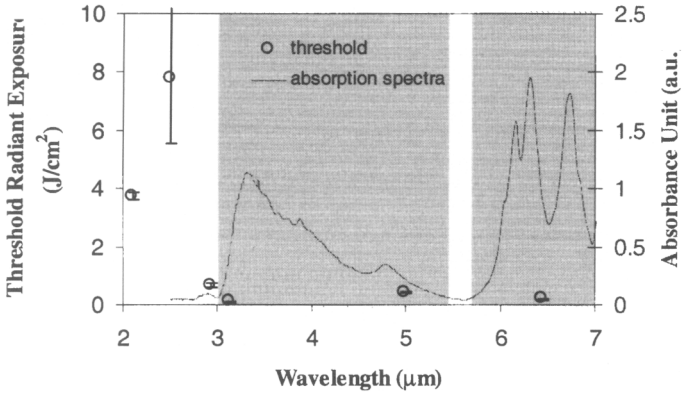

Calculus	Near-IR Absorption Region ($\lambda < 3.0$ μm)	Mid-IR Absorption Region (5.4 μm $< \lambda <$ 5.7 μm)
Cystine	$p = 3.37224 \times 10^{-10}$ ($p < 0.05$)	N/A

FIG. 6. Threshold radiant exposure results for cystine calculus. At top are threshold values and error bars as defined in legend to Figure 3. Absorption spectrum of calculus is superimposed on results. Shaded areas are regions of high optical absorption. At bottom are *P* values for threshold radiant exposures in infrared high-absorption regions compared with near-infrared low-absorption and mid-infrared low-absorption regions. NA = no data available for analysis.

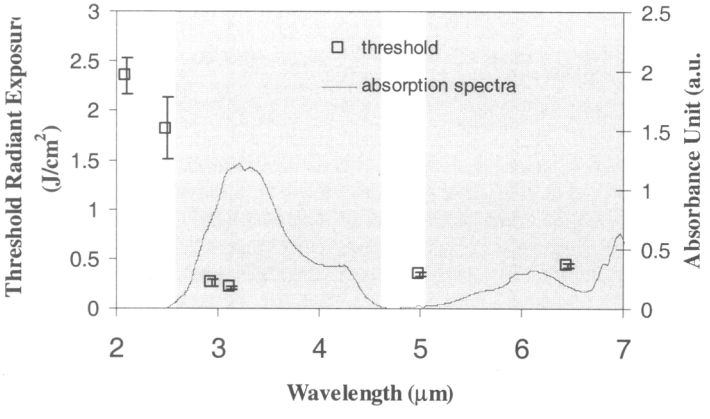

Calculus	Near-IR Absorption Region ($\lambda < 2.6$ μm)	Mid-IR Absorption Region (4.6 μm $< \lambda <$ 5.1 μm)
MAPH	$p = 7.97908 \times 10^{-15}$ ($p < 0.05$)	$p = 0.007526$ ($p < 0.05$)

FIG. 7. Threshold radiant exposure results for MAPH calculus. At top are threshold values and error bars as defined in legend to Figure 3. Absorption spectrum of calculus is superimposed on results. Shaded areas are regions of high optical absorption. At bottom are *P* values for threshold radiant exposures in infrared high-absorption regions compared with near-infrared low-absorption and mid-infrared low-absorption regions.

TABLE 1. THRESHOLD RADIANT EXPOSURES OF VARIOUS URINARY CALCULI AT SIX WAVELENGTHS

Calculus	*2.12 μm*	*2.5 μm*	*2.94 μm*	*3.13 μm*	*5 μm*	*6.45 μm*
Uric acid	3.72	3.79	0.18	0.19	0.50	0.28
COM	7.36	7.20	0.47	0.17	0.79	0.34
Cystine	3.72	7.79	0.66	0.80	0.41	0.18
MAPH	2.33	1.80	0.25	0.20	0.34	0.43

Threshold values are in units of J/cm². Shaded cells designate threshold values in high optical absorption spectral regions.

higher absorption coefficient implies a shorter penetration depth and higher laser fluence within the irradiated volume, assuming constant radiant exposure. Thus, the threshold radiant exposure required to initiate ablation decreases as the absorption coefficient increases. At radiant exposures above threshold, the excess laser energy produces further fragmentation, and hence increasing lithotripsy efficiency. This has been demonstrated in a previous study,[30] in which the lithotripsy efficiencies were markedly higher at 3.13 and 6.1 μm than at 2.12 μm for uric acid and COM calculi.

However, the dependence of threshold radiant exposure on the absorption coefficient is nonlinear. Several discrepancies in the trend predicted by equation 1 are observed. Although we have taken the necessary measures to ensure consistency in our experimental procedure, errors may still occur, as the experiments relied on visual determination. Furthermore, impurities in the sample (which also hindered visual determination because of the inhomogeneous and striated appearance) may contain unknown local chromophores that alter the absorption spectra and thus affect our experimental results. As mentioned earlier, the FEL macropulse consists of a picosecond micropulse train that may affect the laser–calculus interaction. Although the peak power of individual micropulses may not be high enough to generate a significant photomechanical response in the calculus, the influence of pulse structure on ablation threshold cannot be excluded.

Consistently lower threshold radiant exposures at 2.94 μm for all calculus types indicate that laser lithotripsy may be efficiently performed with the Er:YAG laser. With sapphire and other new infrared fibers being approved for endoscopic delivery of the Er:YAG beam, the use of this laser for clinical lithotripsy is worth exploring.

CONCLUSIONS

The threshold radiant exposure for ablation or fragmentation is dependent on the optical absorption of urinary calculi. The threshold radiant exposures are low in the infrared spectral regions where the absorption coefficients are high. Therefore, it may be possible to predict the lithotripsy efficiency on the basis of the optical absorption coefficients of various calculus types.

ACKNOWLEDGMENTS

Funding for this research was supplied in part by grants from the Office of Naval Research Free Electron Laser Biomedical Science Program (N00014-911-J-1564), the Air Force Office of Scientific Research through MURI from DDR&E (F49620-98-1-0480), and the Albert W. and Clemmie A. Caster Foundation.

REFERENCES

1. Watson GM, Wickham JEA, Mills TN, Bown SG, Swain P, Salmon PR. Laser fragmentation of renal calculi. Br J Urol 1983;55: 613–616.
2. Dretler SP. An evaluation of ureteral laser lithotripsy: 225 consecutive patients. J Urol 1989;143:267–272.
3. Mulvaney WP, Beck CW. The laser beam in urology. J Urol 1968;99:112–115.
4. Fair HD. In vitro destruction of urinary calculi by laser-induced stress wave. Med Instrum 1978;12:100–105.
5. Hofmann R, Hartung R, Schmidt-Kloiber H, Reichel E. First clinical experience with a Q-switched neodymium: YAG laser for urinary calculi. J Urol 1989;141:275–279.
6. Dretler SP. Laser lithotripsy: A review of 20 years of research and clinical applications. Lasers Surg Med 1988;8:341–356.
7. Rink K, Delacretaz G, Salathe RP. Fragmentation process induced by microsecond laser pulses during lithotripsy. Appl Phys Lett 1992;61:258–260.
8. Bhatta KM, Nishioka NS. Effect of pulse duration on microsecond-domain laser lithotripsy. Lasers Surg Med 1989;9:454–457.
9. Nishioka NS, Kelsey PB, Kibbi AG, Delmonico F, Parrish JA, Anderson RR. Laser lithotripsy: Animal studies of safety and efficacy. Lasers Surg Med 1988;8:357–362.
10. Spindel ML, Moslem A, Bhatia KS, Jassemnejad B, Bartels KE, Powell RC, O'Hare CM, Tytle T. Comparison of holmium and flashlamp pumped dye lasers for use in lithotripsy of biliary calculi. Lasers Surg Med 1992;12:482–489.
11. Schafer SA, Durville FM, Jassemnejad B, Bartels KE, Powell RC. Mechanisms of biliary stone fragmentation using the Ho:YAG laser. IEEE Trans Biomed Eng 1994;41:276–283.
12. Thomas S, Pensel J, Engelhardt R, Meyer W, Hofstetter AG. The pulsed dye laser versus the Q-switched Nd:YAG laser in laser-induced shock-wave lithotripsy. Lasers Surg Med 1988;8:363–370.
13. Rink K, Delacretaz G, Salathe RP. Fragmentation process induced by nanosecond laser pulses. Appl Phys Lett 1992;61:2644–2646.
14. Rink K, Delacretaz G, Salathe RP. Influence of the pulse duration on laser induced mechanical effects. SPIE Proc 1994;2077: 181–194.
15. Rink K, Delacretaz G, Salathe RP. Fragmentation process of current laser lithotriptors. Lasers Surg Med 1995;16:134–146.
16. Yiu MK, Liu PL, Yiu TF, Chan AYT. Clinical experience with holmium:YAG laser lithotripsy of ureteral calculi. Lasers Surg Med 1996;19:103–106.
17. Razvi HA, Denstedt JD, Chun SS, Sales JL. Intracorporeal lithotripsy with the holmium:YAG laser. J Urol 1996;156:912–914.
18. Das A, Erhard MJ, Bagley DH. Intrarenal use of the holmium laser. Lasers Surg Med 1996;19:103–106.
19. Teichman JMH, Glickman RD, Harris JM. Holmium:YAG percutaneous nephrolithotomy: The laser incident angle matters. J Urol 1998;159:690–694.
20. Dushinski JW, Lingeman JE. High-speed photographic evaluation of holmium laser. J Endourol 1998;12:177–181.
21. Vassar GJ, Teichman JMH, Glickman RD. Holmium:YAG lithotripsy efficiency varies with energy density. J Urol 1998;160: 471–476.
22. Teichman JMH, Vassar GJ, Glickman RD. Holmium:YAG lithotripsy efficiency varies with stone composition. J Urol 1998; 52:392–397.
23. Beghuin D, Delacretaz G, Schmidlin F, Rink K. Fragmentation process during Ho:YAG laser lithotripsy revealed by time-resolved imaging. SPIE Proc 1998;3195:220–224.
24. Chan KF, Vassar GJ, Pfefer TJ, Teichman JMH, Glickman RD, Weintraub SE, Welch AJ. Chemical decomposition of urinary stones during holmium laser lithotripsy I: Lack of a photomechanical effect. SPIE Proc 1999;3601:377–386.
25. Glickman RD, Teichman JMH, Vassar GJ, Pfefer TJ, Weintraub SE, Chan KF, Pfefer TJ, Welch AJ. Chemical decomposition of urinary stones during holmium laser lithotripsy II: Evidence for photothermal breakdown. SPIE Proc 1999;3601:369–376.

26. Vassar GJ, Teichman JMH, Glickman RD, Weintraub SE, Chan KF, Pfefer TJ, Welch AJ. Holmium:YAG lithotripsy: Photothermal mechanism. J Endourol 1999;13:181–190.
27. Chan KF, Pfefer TJ, Welch AJ, Vassar GJ, Teichman JMH, Glickman RD, Weintraub SE. Holmium:YAG laser lithotripsy: A dominant photothermal ablative mechanism with chemical decomposition of urinary calculi. Lasers Surg Med 1999;25(1):22–37.
28. Teichman JMH, Vassar GJ, Bishoff JT, Bellman GC. Holmium:YAG lithotripsy yields smaller fragments than pulsed dye, Lithoclast, or electrohydraulic lithotripsy. J Urol 1998;159: 18–27.
29. Daidoh Y, Arai T, Komine Y, et al. Determination of optimum wavelength for laser photofragmentation of urinary stones. J Endourol 1991;5:245–249.
30. Chan KF, Hammer DX, Vargas G, et al. Free electron laser ablation of urinary calculi: A Preliminary Study [abstract 1430]. J Urol 1999;161(suppl):369.
31. Welch AJ, van Gemert MJC (eds): Optical-Thermal Response of Laser-Irradiated Tissue. New York: Plenum Press, 1995, p 722.
32. Khosrofian JM, Garetz BA. Measurement of a Gaussian laser beam diameter through the direct inversion of knife-edge data. Appl Optics 1983;22:3406–3410.
33. Cain CP, Noojin GD, Manning L. A comparison of various probit methods for analyzing yes/no data on a log scale. USAF Armstrong Laboratory Technical Report AL/OE-TR-1996-0102, 1996.
34. Dao NQ, Daudon M. Infrared and Raman Spectra of Calculi. Paris: Elsevier, 1997.
35. Long FH, Nishioka NS, Deutsch TF. Measurement of the optical and thermal properties of biliary calculi using pulsed photothermal radiometry. Lasers Surg Med 1987;7:461–466.

Address reprint requests to:
Kin Foong Chan, M.S.E.
Dept. of Electrical and Computer Engineering
University of Texas at Austin
ENS610
Austin, TX 78712

E-mail: kfchan@ccwf.cc.utexas.edu